Egyptian Informatics Journal (2013) **14**, 117–123

Cairo University

Egyptian Informatics Journal

www.elsevier.com/locate/eij
www.sciencedirect.com

ORIGINAL ARTICLE

An efficient super-resolution approach for obtaining isotropic 3-D imaging using 2-D multi-slice MRI

Alaa A. Hefnawy *

Computer & Systems Dept., Electronics Research Institute, El-Tahrir St., Dokki, Cairo, Egypt

Received 19 November 2012; accepted 31 March 2013
Available online 19 April 2013

KEYWORDS

Multi-slice magnetic resonance imaging (MRI); Super-resolution; Regularized MAP

Abstract An approach for obtaining both a high-resolution and high-contrast 3D MRI image volume, desirable for image-guided minimally invasive brain surgery, is proposed. Current MRI imaging techniques, especially in situations where contrast requirements dictate use of T2- weighed sequences with long repetition times, do not deliver sufficient resolution in the cross-slice direction. As SRR techniques can be very attractive for obtaining isotropic 3D MRI images from the anisotropic 2D multi-slice volumes, we adopt in this work a MAP super-resolution method with modified regularization parameters. Experiment results demonstrate that resolution enhancement and better edge definition are obtained.

1. Introduction

A common goal in all medical imaging systems is to increase the resolution and, to the extent possible, achieve true isotropic 3D imaging. To accomplish this goal, various imaging modalities have been developed over the years, each based on a particular energy source that passes through the body [1]. High resolutions and high contrast, isotropic 3D magnetic resonance imaging (MRI) images, is noninvasive important tool for visualizing the body's internal soft tissues (brain, muscles, heart, and tumors) and for early medical diagnosis. MRI works to collect data in either a 3D volumetric fashion using phase encoding in slice direction or as a set of 2D multi-slice acquisition. Although true 3D Fourier acquisition is often the preferred approach in MRI applications where high resolution in three dimensions is required, this option is not available in practice for all desired image contrast mechanisms. For example, in very well-known and popular MRI strategies, such as the inversion recovery method and T_2-weighted fast spin echo imaging, the long repetition times, in both methods, push imaging times for 3D acquisition imaging beyond practical limits [2]. When the true 3D image acquisition is not effective or possible, it is common practice to acquire a set of 2D slices. For MRI strategies with long repetition times (and in consequence, are not easily compatible with true 3D spatial Fourier encoding), interleaved multi-slice acquisition can obtain contiguous 3D spatially resolved data much more efficiently and remains the most popular choice in clinical practice [3].

However, the problem is that a set of 2D slices does not give a good isotropic 3D image. A reconstructed MR image is

* Tel.: +20 33310502 (O), +20 39745098 (H).
E-mail addresses: alaahouse@yahoo.com, alaa@eri.sci.eg

Peer review under responsibility of Faculty of Computers and Information, Cairo University.

ELSEVIER Production and hosting by Elsevier

1110-8665 © 2013 Production and hosting by Elsevier B.V. on behalf of Faculty of Computers and Information, Cairo University.
http://dx.doi.org/10.1016/j.eij.2013.03.003

commonly of high-resolution in-plane (x, y) and of much reduced resolution in the slice-select (z) direction. The minimum practical slice thickness for such techniques is approximately 1.5–2 mm. Thinner slices generally suffer severe degradation in signal-to-noise ratio (SNR), even on high-field (3 T) scanner instruments [4]. To overcome the poor resolution in the slice-selection direction in 2D multi-slice imaging, algorithms for resolution enhancement have been explored, based on the super-resolution reconstruction (SRR) concept [2–10].

SRR is commonly defined as the idea of creating a high-resolution (HR) image from several low resolution (LR) images of the same scene taken at different viewpoints [11,12]. Recently, research in super-resolution restoration has gained high interest, due to the increasing availability of computational power and larger memories in computing technology.

In fact, this reconstruction process is typically an ill-posed problem, which means a small perturbation in the input would produce a huge unexpected disturbance in the output. A variety of regularization techniques have been proposed, such as half-quadratic regularization (HQR) [13], directional regularization [14], and adaptive regularization [15]. Nevertheless, Tikhonov regularization is still one of the most commonly used methods to solve the ill-posed problem because of easy implementation and speed. The regularization is used to form a constraint and transforms the problem into a minimization. Though it has such advantages in implementation, the resulting image is often not able to preserve edges and possibly affected by a global smoothness and even ringing artifacts. An explanation of the phenomenon is attributed to the regularization parameter, which manages the degree to which the regularization is performed on the problem. Choosing appropriate regularization parameters has been discussed in [16].

In this paper, we introduce an efficient approach for recovering HR isotropic 3D MRI image volume. We used the Shilling's et al. [4] multi-stack approach for data acquisition model that depends on combining multiple 2D multi-slice stacks of MRI images with different scanning orientations. Here, instead of using the projection onto convex sets (POCS) method (as in [4]) to solve the super-resolution reconstruction problem, we use a Maximum a posteriori optimizer with adaptive local regularization parameters.

2. Theory

2.1. SR algorithms

Super-resolution reconstruction (SRR) is the process of fusion a sequence of LR noisy blurred images to produce a higher resolution image or sequence. The information that was gained in the SR-image was embedded in the LR images in the form of aliasing. That is, LR images are sub-sampled (aliased) as well as shifted with sub-pixel precision. Initial image resolution is based on the properties of the sensor. The sensor can vary from common cameras, satellites, SAAR radars, MR devices, etc. Each sensor has its own characteristics that affect the images it produces.

In restoration theory [2], the N measured images can be lexicographically ordered into the vectors $\{\underline{Y}_k\}_{k=1}^{N}$, each modeled from the single high-resolution image $\underline{X}$. Each measured image is represented by a geometric transform of the desired high-resolution image, blurring, and then sampling with additive noise $\underline{E}_k$. This can be expressed as

$$\underline{Y}_k = D_k C_k F_k \underline{X} + \underline{E}_k \tag{1}$$

where D_k, C_k, and F_k are the down sampling, blurring, and geometry operators for the kth measurement, respectively. Grouping the equations allows for the classic restoration problem

$$\begin{bmatrix} \underline{Y}_1 \\ \vdots \\ \underline{Y}_N \end{bmatrix} = \begin{bmatrix} D_1 C_1 F_1 \\ \vdots \\ D_N C_N F_N \end{bmatrix} \underline{X} + \begin{bmatrix} \underline{E}_1 \\ \vdots \\ E_N \end{bmatrix} \Longleftrightarrow \underline{Y} = \mathrm{H}\underline{X} + \underline{E} \tag{2}$$

If the number of measurements is much less than the number of ideal image pixels, then the problem of image recovery is under-determined and cannot be recovered completely. Conversely, if the measurements greatly exceed the number of ideal image pixels, then the system may over-determined and noise will be attenuated but information will be disregarded. For a fully determined system, the number of independent measurements should be greater than the number of image pixels in the restored image.

In initial works [17], the frequency domain was used to demonstrate the ability to reconstruct one improved resolution image from several down-sampled noise free versions of it, based on the spatial aliasing effect. The frequency domain approach was further generalized to noisy and blurred images in [18], and a spatial domain alternative was suggested in [19]. Further, noniterative spatial domain data fusion approaches were proposed in [20,21]. An iterative back-projection (IBP) method was proposed in [22]. This method starts with an initial guess of the outcome image, projects the initial result to simulate the LR measurements, and updates the temporary guess according to the simulation error. A set theoretic approach to SR was suggested in [23] where, convex sets are defined, which represent tight constraints on the required image. Nonlinear constraints are combined within the restoration process and a POCS algorithm is utilized. A hybrid model that combines maximum-likelihood (ML) and POCS was suggested in [2]. More recent SR works aim at combining the SR approaches with regularization terms, e.g. in [24] fast and robust multi-frame SR is proposed using L_1 norm minimization and robust regularization based on a bilateral prior to deal with different data and noise models.

2.2. SR in MRI

In 2D multi-slice acquisition, reconstructed 3D MR images are commonly of HR in-plane (x, y) and of much reduced resolution in the slice-select (z) direction. For example, it is common to find reconstructed 3D MR images of size $1 \times 1 \times 3$ mm^3. The spatial resolution in-plane (x, y) is determined by several factors, including the gradients' intensity, the imaging bandwidth, the number of 'readout' points and phase encoding steps [2]. The slice thickness in MRI is determined by what is termed the slice-selection pulse, which is in turn determined by hardware limitations coupled with pulse sequence timing considerations.

Previously, several attempts have been made to improve the resolution of MR images. The methods of Peled et al. [25] and Carmi et al. [5] try to improve the in-plane resolution. The

validity of such methods was questioned by Scheffler [26]. The Fourier-encoded in-plane data (i.e. phase- or frequency encoding) given by the MR device are inherently band limited. This is due to the time limit of the acquisition process and the fact that the information is gathered in the frequency domain (known as 'k-space' acquisition). As elucidated by Scheffler, this prevents recovery of any high spatial frequency content by repeated sampling at different locations. In-plane shifting is thus equivalent to a global phase shift in the acquisition space (k-space), the original temporal domain, which does not affect the inherent spatial frequency resolution of the acquired data.

A different scenario exists in the slice-select direction of a Fourier-encoded MRI. There is sufficient information in the slice-select dimension such that under-sampling of the data in that direction results in aliasing. A less sharp cut-off can thus be observed when viewing the spatial frequencies in the slice-select (z) direction in Fourier encoded MRI. The existing aliasing in the slice-select direction provides the basis for using SR algorithms to augment the resolution.

For SRR to work in MRI, the different viewpoints may correspond to a combination of different scanning offsets, orientations, or sampling periods. Successful SRR approach in MRI was proposed by Greenspan et al. [9], for reconstruction of a HR data volume, by combining multiple overlapping parallel lower-resolution image stacks, spaced equidistantly across the slice normal direction at a fraction of the slice distance. They validated the slice offset approach by showing new spectral content beyond the LR scans. A variant to ensure localized errors in the SRRs was proposed by Carmi et al. [5]. Shilling et al. [4] showed that the reconstruction from multiple slice stacks at different slice orientations (i.e. rotated around a common frequency encoding axis) outperforms the reconstruction from multiple parallel overlapping slice stacks at sub-pixel location offsets.

The challenge for SR in MRI is to increase the resolution in the slice-select dimension (i.e. reducing the slice thickness) so as to achieve HR, isotropic, 3-D images. A further challenge is to achieve the HR outcome without decreasing the SNR. While SRR in MRI is a developing field, showing its potential in resolution enhancement, a major question from the MRI community is whether SRR has any advantage over direct HR 3D acquisition when SNR and acquisition times are taken into account. Using extensive analysis, Plenge et al. [6], have proofed (through evaluation framework) that SRR is capable of providing better trade-offs between resolution, SNR and acquisition time than direct HR 3D acquisition. Moreover, they have compared the performance of many SRR in MRI methods, concluded that while the Tikhonov regularization-based method gives the highest resolution, the POCS yields the over-all poorest resolution results.

3. Model

3.1. The data model

The multi-stack approach combines multiple 2-D multi-slice scans or stacks as shown in cross section in Fig. 1. Except for slice orientation, all scans share the same acquisition parameters. The data input conditions are as follows:

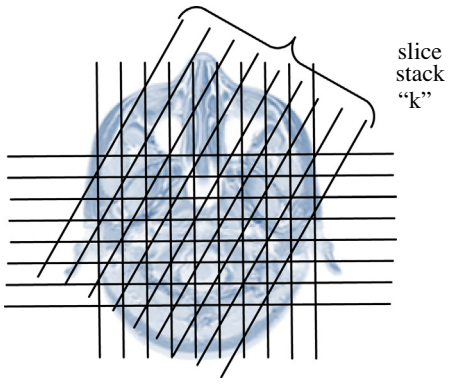

Figure 1 Multiple slice stack orientations.

- Slices are equidistant and parallel within each slice stack, and have identical slice selection profiles.
- Slice centers in each stack are aligned along the slice plane normal.
- The slice orientations are at equal angular sampling intervals. The same read out direction across all stacks, orthogonal to the planes shown in Fig. 1 results in consistent chemical shift artifacts which can thus be ignored for reconstruction in this direction.
- Scans are spatially co-registered.
- Contrast parameters are equal.

Under these conditions the problem of reconstructing a 3-D data volume from a set of such slice stacks possesses translational symmetry along the readout direction. Thus, the problem is reduced to a series of identical 2-D inversion problems with different measurement data.

The input to the multi-stack image reconstruction consists of the individual image stacks after Fourier reconstruction. The scanning (or slice excitation) direction for the kth stack undergoes a coordinate transformation (geometry warping as indicated in Eq. (1)) by a rotation matrix, $R_k \in SO(3)$. The slice-selective excitation process is modeled by a convolution of the image by a slice profile function, followed by uniform sampling described by a diagonal sampling matrix V. The diagonal structure of V represents a rectangular sampling process. The LR image, $y_k[n]$, from the kth stack at discrete image coordinate, $n \in \mathbb{Z}^3$, is related to the HR image, $x(s) : \mathbb{R}^3 \to \mathbb{C}$, by

$$y_k[n] = \int_{\Omega} x(s)h(R_k(s - V_n))ds \tag{3}$$

where $\Omega \in \mathbb{R}^3$ is the region of support for x(s) and h(s) is the slice selection function. Sampling followed by a lexicographical ordering of $y_k[n]$ creates the LR image vector $\mathbf{y}$ by replacing stack index k and sampled location indices $\mathbf{n}$ with a composite pixel index i[1]. The measurements can then be ordered into the data vector $\mathbf{y}$ giving the linear system

$$\mathbf{y} = Hx \tag{4}$$

The dimensions of H dictate the maximum possible resolution improvement of the HR image. In this case, $H \in \mathbb{R}^{\mathbb{M}\times\mathbb{N}}$, and will be a sparse matrix. Here, M and N are the total number of measurements and unknowns, respectively. The isotropic voxel size of the HR image must allow H to be nonsingular. This means $M \geqslant N$. If the in-plane resolution

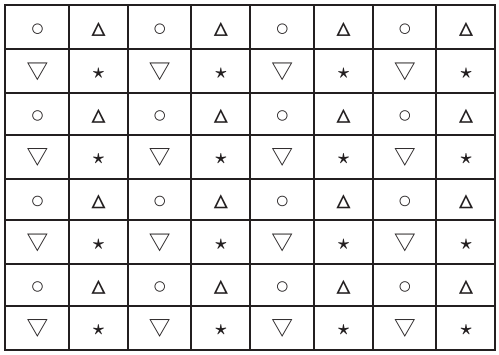

Figure 2 The diagram of a preliminary HR image; ○ is an element in the first LR image, △ the second LR, ▽ the third LR image and ★ the fourth one.

of the LR slices is equal and isotropic and the number of stacks is greater than or equal to the slice thickness (expressed in number of LR pixels), then the SRR will have isotropic resolution. If there are K stacks, S slices per stack, and P voxels per stack in the phase-encoding direction then $M = KSP$ and the necessary condition for signal recovery becomes

$$N \leqslant KSP \tag{5}$$

The real and imaginary components of the intrinsically complex-valued MRI data in x(s) are each independently corrupted by Gaussian noise. Therefore, in this work we relied on using stochastic estimator such as maximum a posteriori (MAP) in the reconstruction [27].

3.2. The solution of the inverse model (reconstruction process)

Solving the model of (4) to determine x from Q observations of y and knowledge of H, is a typical ill-posed inverse problem. Procedures adopted to stabilize the inversion of ill-posed problem are called *regularization*. Through the regularization, using the MAP estimator (under the assumption that the error between frames is independent and the noise is an independent identically distributed zero mean Gaussian distribution), the optimization problem for (4) can be written as of seeking an estimate x to minimize the Lagrangian:

$$\widehat{X} = arg\min_x \left[\sum_{k=1}^{Q} ||y_k - H_k \hat{X}||2^2 + \lambda ||TX||_2^2 \right] \tag{6}$$

This widely employed form of regularization, known as Tikhonov regularization [28], where the operator T is generally a high-pass filter, and $||\cdot||$ represents L_2 norm. The coefficient λ represents the Lagrange multiplier, commonly referred to as the regularization parameter. It controls the tradeoff between fidelity to the data (as expressed by the first term), and smoothness of the solution (as expressed by the second term). T is often chosen as the Laplacian operator to smooth the solution. So the minimizer of (6) can be expressed as the normal equation

$$H^T y = (H^T H - \lambda T^T T)x \tag{7}$$

The solution of the above equation is numerically feasible only by iterative methods even for modest image sizes. This leads to the following iteration equation

$$\widehat{X}^{n+1} = \hat{X}^n + \beta \left[\sum_{k=1}^{q} H_k^T (y_k - H_k \widehat{X}^n) - \lambda T^T T \widehat{X}^n \right], \tag{8}$$

where β represents the convergence parameter. Convergence is satisfied when $\beta \in [0, 2]$,

4. Method

4.1. The modified regularization parameter

The regularization parameter λ controls the degree of regularization on the reconstruction. The Larger values of λ will generally lead to a smoother solution. This is useful when only a small number of LR images are available (the problem is under-determined) or the fidelity of the observed data is low due to registration error and noise. On the other hand, if a large number of LR images are available and the amount of noise is small, small λ will lead to a good solution. Generally speaking, choosing λ could be either done manually, using visual inspection, or automatically using methods like discrepancy principle, generalized cross-validation and the L-curve [29].

Here, we propose to determine it according to the local gradient of a *preliminary* HR image. We can form a preliminary HR image through reorganizing the pixel values of the LR

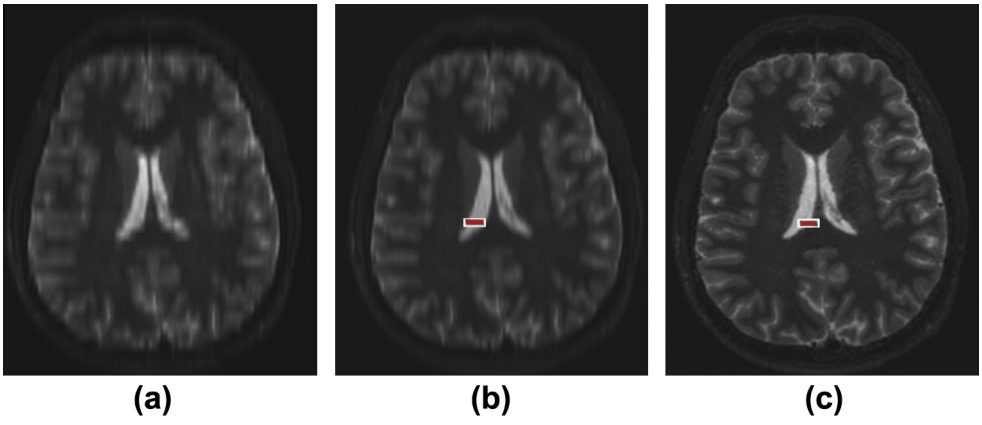

Figure 3 (a) Reformat through a single slice stack, (b) SRR using Tikhonov regularization, and (c) SRR using the proposed method.

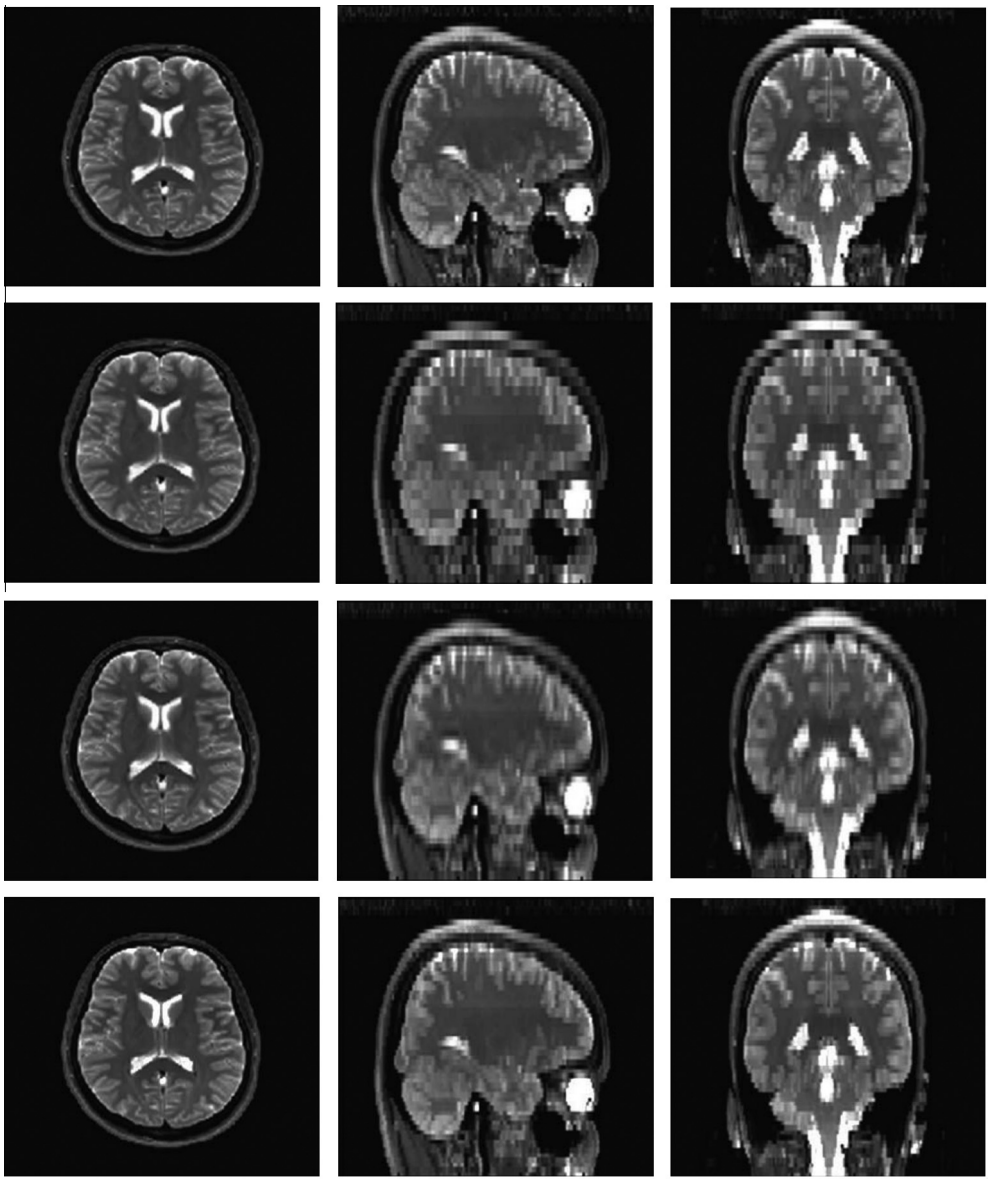

Figure 4 Top raw: HR T2-w volume, Second raw: downsampled LR version, Third raw: SRR using POCS, Bottom raw: SRR using the proposed method.

images. Let us assume for simplicity that we have four LR images, the preliminary HR image can be constructed as shown in Fig. 2, where ○, △, ▽ and ★ represent elements in the four LR images, respectively.

This is different from the one, generally used, in regularization methods. Most of them use a global parameter to regularize the whole image. Here the parameter is a vector and *i*th element weights the regularization on *xi*, *i*th element in *x*. Its configuration is related to the magnitude of the gradient vector field of the preliminary HR image and estimated by the expression:

$$\lambda_i = \lambda_{\min}[1 - \exp(-\alpha|\nabla x_i|)] + \lambda_{\max}\exp(-\alpha|\nabla x_i|), \quad (9)$$

where $|\nabla x_i|$ stands for the magnitude of gradient vector at x*i*, α controls the rate of exponential decrease, and $\lambda_{\min}$ and $\lambda_{\max}$ are the minimal and maximal values of the parameter. When a reconstructed image is over smoothed, the regularization parameter is chosen as the maximum $\lambda_{\max}$. When the image is too rough, the parameter corresponds to the minimum $\lambda_{\min}$. Combining properties of MR medical images, we can evaluate an appropriate value for every element of the parameter through three factors, α, $\lambda_{\min}$, and $\lambda_{\max}$. Local gradient information is utilized to determine where and to what degree of regularization should be imposed, which is advantageous at restoring local edges and suppressing noise according to local information.

4.2. The experimental design

4.2.1. Real clinical data (in vivo brain scan)

Using a 3-T Siemens Trio/TIM scanner, a set of six equidistantly spaced angles scans was acquired with the following parameters: Multi-slice Inversion-Recovery Fast Spin-Echo (IR-FSE), (TE/TI/TR) = (85/190/4830) ms, flip angle = 90°, 512×512 pixels image grid on a 220 mm in-plane square

field-of-view (FOV); slice thickness = 4.8 mm with in-plane resolution = 0.8 mm, (i.e. voxel size = 4.8 mm × 0.8 mm × 0.8 mm); scan time 3 min/stack. The readout direction is orthogonal to the transverse plane and the angle between adjacent slice stacks is 30°.

4.2.2. Experimental data

To validate the proposed method, a synthetic data set was used. High-resolution T2-w data set from the publicly available *Brain web* database was used [30]. The HR T2-w volumes have 256 × 256 × 56 voxels with a voxel resolution of 1 mm^3 in 1.5-T scanner. Six slice stacks with 30° increments HR T2-w volumes were down sampled in the z direction to a voxel resolution of 1 mm × 1 mm × 3 mm (i.e., slice thickness = 3 mm), to form the LR data. Both the projection onto convex sets (POCS) method and the proposed method were used to reconstruct the LR volumes to resolution of 1mm3. The Peak Signal-to-Noise Ratio (PSNR) measure was used to compare the reconstructed data and the reference HR data.

5. Results

5.1. Real clinical data

5.1.1. Qualitative analysis

An axial reformat through one of six sagittal LR in vivo brain scans is shown in Fig. 3a for reference. Fig. 3b and c shows the SRR using the traditional Tikhonov regularization method and the proposed method (modified Tikhonov regularization), respectively. The SR reconstructed images show excellent anatomical details compared to the LR image. The isotropic voxel size of the resultant reconstructed volume is 0.8 mm × 0.8 mm × 0.8 mm. Moreover, modified regularization reconstruction has a better contrast than the common Tikhonov regularization, which allow for good discrimination of cortical and deep-brain gray matter.

5.1.2. Quantitative analysis

The resolution was quantified by the measurement of the edge sharpness of the images (as the edges play a critical role in medical imaging) [31]. The mathematical formula has been suggested by Greenspan et al. [9]. The width of each edge is measured by least-squares fitting it to a sigmoid function of the form:

$$f(q) = \frac{1}{1 + \exp(-\gamma(q - \delta))} \tag{10}$$

The parameter γ is inversely proportional to the width, and δ corresponds to the center location. Following the fitting step, a measure of "rise length" is computed, defined as the width (in high-resolution pixels) from 10% to 90% of the edge height. It is easy to show that:

$$\text{width[pixel]} = \frac{4.4}{\gamma} \tag{11}$$

To quantify the resolution augmentation, the edge width was calculated in the highlighted position in Fig. 3, for the LR, SRR with Tikhonov estimate, and SRR with modified Tikhonov estimate. The measured edges were 4.8, 2.9, and 2.4, respectively.

5.2. Experimental data

A comparison of the LR views in Fig. 4 (second raw) with the corresponding both SRR techniques (third and bottom raw) clearly illustrates the resolution improvement in the slice selection direction (coronal and sagittal views).

To evaluate the used reconstruction methods, the PSNR has been computed. The mean squared error (MSE) of the reconstructed image $f(i,j)$ is

$$\text{MSE} = \frac{\sum[f(i,j) - f_0(i,j)]^2}{\text{Image size}} \tag{12}$$

where $f_o(i,j)$ is the HR image. The root mean squared error (RMSE) will be the square root of MSE. PSNR is measured by using

$$\text{PSNR} = 20\ \log_{10}\left(\frac{255}{\text{RMSE}}\right) \tag{13}$$

The reconstruction using the POCS method obtained a PSNR equal to 29.5 dB and the proposed method 33.6 dB. In Fig. 4, the different results can be visually compared. One can see that the reconstruction using the proposed approach not only obtained a better PSNR value than the POCS method but also showed a better anatomical content.

6. Conclusions

We have presented an efficient approach to merge multiple MRI scans under a super-resolution framework. The technique depends on combining multiple MRI scans with different slice orientations (which offers a more natural avenue toward isotropic image resolution than multiple acquisitions at the same orientation with sub-pixel offsets), using a super-resolution algorithm with adaptive regularization parameter. The result of experiment has shown an outstanding resolution augmentation of the reconstructed isotropic 3D MRI volume. The modified regularization parameters method has proven to preserve the edges and improve the sharpness.

References

[1] Bourne Roger. Fundamentals of digital imaging in medicine. Springer; 2010.
[2] Greenspan. Super-resolution in medical imaging. Comput J 2009;52:43–63.
[3] Shilling R, Mewes K, Brummer M. Merging multiple stacks MRI into a single data volume. IEEE ISBI 2006.
[4] Shilling RZ, Robbie TQ, Bailloeul T, Mewes K, Mersereau RM, Brummer ME. A super-resolution framework for 3-D high-resolution and highcontrast imaging using 2-D multislice MRI. IEEE Trans Med Imag 2009;28:633–44.
[5] Carmi E, Liub S, Alona N, Fiata A, Fiat D. Resolution enhancement in MRI. Magn Reson Imag 2006;24:133–54.
[6] Plenge E, Poot DHJ, et al. Super-resolution methods in MRI: Can they improve the trade-off between resolution, signal-to-noise ratio, and acquisition time? Magn Reson Med. doi: 10.1002/mrm.24187, 2012.
[7] Gholipour A, Estroff JA, Warfield SK. Robust super-resolution volume reconstruction from slice acquisitions: application to fetal brain MRI. IEEE Trans Med Imag 2010;29(10):1739–58.
[8] (a) Gholipour A et al. Maximum A Posteriori Estimation of Isotropic High-Resolution Volumetric MRI from Orthogonal

Thick-Slice Scans. Lecture Notes in Computer Science 2010;6362/2010:109–16, doi: 10.1007/978-3-642-15745-5_14;
(b) Elad M, Feuer A. Restoration of a single superresolution image from several blurred, noisy, and under sampled measured images. IEEE Trans Image Process 1997;6:646–1658.
[9] Greenspan H, Oz G, Kiryati N, Peled S. MRI interslice reconstruction using super-resolution. Magn Reson Imag 2002;20:437–46.
[10] Shilling Richard Z, Ramamurthy Senthil, Brummer Marijn E. Sampling strategies for super-resolution in multi-slice MRI. ICIP 2008:2240–3.
[11] Park SC, Park MK, Kang MG. Super resolution image reconstruction – a technical overview. IEEE Signal Process Mag 2003, May.
[12] Hefnawy A. Super resolution challenges and rewards, chapter 6 of 'intelligence for nonlinear dynamics and synchronisation'. Atlantis Press; 2010.
[13] Deriche R, Kornprobst P, Nikolova M, Ng M. Half-quadratic regularization for MRI image restoration. In: Proceedings of 2003 IEEE international conference on acoustics, speech and signal processing, vol. 6; April 2003. p. 585–8.
[14] Lee S, Cho H, Park J-I. Directional regularisation for constrained iterative image restoration. Electron Lett 2003;39(23):1642–3.
[15] Choi Y-S, Shin H-C, Song W-J. Adaptive regularization matrix for affine projection algorithm. IEEE Trans Circuits Syst II, Exp Briefs 2007;54(12):1087–91.
[16] Oraintara S, Karl WC, Castanon DA, Nguyen TQ. A method for choosing the regularization parameter in generalized tikhonov regularized linear inverse problems. In: International conference on image processing, October 2000. p. 93–6.
[17] Tsai RY, Huang TS. Multipleframe image restoration and registration. In: Advances in computer vision and image processing. Greenwich, CT: JAI Press Inc.; 1984. p. 317–39.
[18] Kim SP, Bose NK, Valenzuela HM. Recursive reconstruction of high resolution image from noisy undersampled multiframes. IEEE Trans Acoust, Speech, Signal Process 1990;38:1013–27, June.
[19] Ur H, Gross D. Improved resolution from subpixel shifted pictures. Computer Vis Graph Model Image Process 1992;54:181–6.
[20] Elad M, Hel-Or Y. A fast super-resolution reconstruction algorithm for pure translational motion and common space invariant blur. IEEE Trans Image Process 2001;10:1187–93.
[21] Chiang MC, Boult TE. Efficient super-resolution via image warping. Image Vis Comput 2000;18:761–71.
[22] Irani M, Peleg S. Motion analysis for image enhancement: resolution, occlusion, and transparency. J Vis Commun Image Represent 1993;4:324–35.
[23] Patti AJ, Sezan MI, Tekalp AM. High-resolution image reconstruction from a low-resolution image sequence in the presence of time-varying motion blur. In: Proc. ICIP, Austin, TX; 1994. p. 343–7.
[24] Farsiu S, Robinson MD, Elad M, Milanfar P. Fast and robust multiframe super resolution. IEEE Trans Image Process 2004;13:1327–44.
[25] Peled S, Yeshurun H. Superresolution in MRI: application to human white matter fiber tract visualization by diffusion tensor imaging. Magn Reson Med 2001;45:29–35.
[26] Scheffler K. Superresolution in MRI? Magn Reson Med 2002;48:408.
[27] Hardie RC, Barnard KJ, Armstrong EE. Joint MAP registration and high-resolution image estimation using a sequence of undersampled images. IEEE Trans Image Process 1997;6(December):1621–33.
[28] Tikhonov AN, Arsenin VY. Solutions of Ill-posed problems. Washington, DC: V.H. Winston & Sons; 1977.
[29] Kilmer M, O'Leary D. Choosing regularization parameters in iterative methods for ill-posed problems. SIAM J Matrix Anal Appl 2001;22(4):1204–21.
[30] http://brainweb.bic.mni.mcgill.ca/brainweb/.
[31] Ziye Yan, Yao Lu. Super resolution of MRI using improved IBP. In: International conference on computational intelligence and security, vol. 1; 2009. p. 643–7.